

## Adsorption and Inhibitive Properties of *Ruta chalepensis* L. Oil as a Green Inhibitor of Steel in 1 M Hydrochloric Acid Medium

A. Khadraoui<sup>1\*</sup>, A. Khelifa<sup>1</sup>, H. Boutoumi<sup>1</sup>, H. Hamitouche<sup>1</sup>, R. Mehdaoui<sup>1</sup>, B. Hammouti<sup>2,3</sup>, S.S. Al-Deyab<sup>3</sup>

<sup>1</sup> Laboratoire de Génie chimique, Département de Chimie Industrielle, Faculté de Technologie, Université Saâd Dahlab de Blida, BP 270, Route de Soumaâ, 09000, Blida, Algeria.

<sup>2</sup> LCAE-URAC18, Faculté des Sciences, Université Mohammed Premier, BP 4808, Oujda, Morocco.

<sup>3</sup> Petrochemical Research Chair, Department of Chemistry, College of Science, King Saud University, B.O. 2455, Riaydh 11451, Saudi Arabia

\*E-mail: [hammoutib@gmail.com](mailto:hammoutib@gmail.com)

Received: 16 November 2013 / Accepted: 11 March 2014 / Published: 23 March 2014

---

Inhibition of steel corrosion by *Ruta chalepensis* L. oil has been investigated in aqueous 1 M hydrochloric acid solution using weight loss method, potentiodynamic polarization, electrochemical and impedance spectroscopy (EIS). The inhibition efficiency of *R. chalepensis* L. oil was calculated and compared. We note good agreement between these methods. The results obtained revealed that the inhibitor tested reduce differently the kinetics of corrosion process of steel. Its efficiency increases with the concentration and attained 77% at 2.5 ml/L. Effect of temperature on the corrosion behavior of steel in 1M HCl was also studied in the range 308 K and 338 K. The thermodynamic data of activation are determined. The analysis of *R. chalepensis* L. oil, obtained by steam distillation, using Gas Chromatography (GC) and Gas Chromatography/Mass Spectroscopy (GC/MS) showed that the major components were 2-Undecanone (67 %), 2-Decanone (9 %), 6-(3',5'-Benzodioxyl)-2-hexanone (6.3 %) and 2-Dodecanone (4 %).

---

**Keywords:** Corrosion; Green Inhibitor; *Ruta chalepensis* L. essential oils; Adsorption

### 1. INTRODUCTION

The study of steel corrosion phenomena has become an industrial and academic topic in recent years. Particularly in acidic media, because of the increased industrial applications of acid solutions; Such as, the acid pickling, industrial cleaning, acid descaling, oil well acid in oil recovery and the petrochemical processes [1,2]. Among the acid solutions, hydrochloric acid is one of the most widely used agents.

A large number of synthetic organic compounds were studied as corrosion inhibitors for steel [3–6]. The adsorption modes of these inhibitors depend mainly on the chemical structure of the inhibitor, the chemical composition of the solution, the nature of the metal surface and the electrochemical potential of the metal-solution interface.

Temperature effects on acidic corrosion and corrosion inhibition of steel most often in acidic solutions had been the object of a large number of investigations [7–11]. Temperature dependence of the inhibitor efficiency and the comparison of the obtained thermodynamic data of the corrosion process both in absence and presence of inhibitors lead to some conclusions concerning the mechanism of inhibiting action.

Then, it has been found that certain organic substances containing polar functions with nitrogen, sulphur and/or oxygen atoms in the conjugated system have been reported to exhibit good inhibiting properties of steel in acidic environment [12-19]. The results of all these studies suggest that the inhibitory behavior of the organic compounds subsists in some chemical species or molecules in the inhibiting substances forming a protective layer between the metal surface and the corrodent. The adsorbate layer formed isolates the metal surface from the corrodent thereby reducing the corrosion rate of the metal surface. The toxic nature of these organic inhibitors has required research activities in recent times toward finding alternative environmentally friendly acid corrosion inhibitors.

Natural products were previously used as corrosion inhibitors for different metals in various environments [20, 21] and their optimum concentrations were reported. The obtained data showed that plant extracts could serve as effective corrosion inhibitors and they have become important because they are environmentally acceptable, readily available and renewable source for a wide range of needed inhibitors. Plant extracts are viewed as an incredibly rich source of naturally synthesized chemical compounds that can be extracted by simple procedures with low cost. The extracts from the leaves, seeds, heartwood, bark, roots and fruits of plants have been reported to inhibit metallic corrosion in acidic media [22-27].

These advantages have incited us to examine natural substances as corrosion inhibitors such as: *Rosemary* oil [28-30], *Thymus* oil [31,32], *Artemisia* [33-35], *Lavender* oil [36], *Jojoba* oil [37], *Pennyroyal Mint* oil [38], *Argania* [39-40] and *prickly pear seed* oil [41]. It has been established that the inhibitory actions of plant extracts are due to the presence of some organic compounds such as saponin, tannin, alkaloid, steroids, glycosides, and amino acids. Most of these compounds have centers for  $\pi$ -electrons and functional groups which provide electrons that facilitate the adsorption of the inhibitor on the metal surface. Also, the presence of hetero atoms such as N, P, O, and S enhances the adsorption (which is the initial mechanism of inhibition) of the inhibitor on the metal surface.

In Algeria, collection of medicinal and aromatic plants to extract, after distillation, essential oils for the manufacture of cosmetics, pharmaceuticals as well as flavors for food products, is a virgin field. The distillation of plants is sufficiently known, but remains largely untapped, despite the availability in Algeria of large tracts of forests and fields, whose territory covers important plant resources distributed on the coasts, plains, mountains, steppes, the Sahara and around water points.

*Ruta. chalepensis* L. oil has not been used as a corrosion inhibitor for steel. It is a native and perennial aromatic herb of the Mediterranean region [42] but it is widely growing in many parts of the world in temperate and tropical countries, *R. chalepensis* L. is used in the traditional medicine for

treatment of variable diseases. This plant is described for its emmenagogue, antispasmodic rubfiant, and escharotic powder. *R. chalepensis* L are sources of diverse classes of natural products such as flavonoids, alkaloids, essential oils, coumarins, phenols, saponins, lignans, and triterpenes, with biological activities including antifungal, antioxidant, phytotoxic, abortive, depressant, antidotal and anti-inflammatory [43-46].

In the present work, inhibitive action of *R. chalepensis* L. Oil as a cheap, eco-friendly and naturally occurring substance on corrosion behavior of steel in 1M HCl has been investigated through weight loss measurements, potentiodynamic polarization and electrochemical impedance spectroscopy (EIS) methods. This study aimed also to investigate the temperature effects on steel corrosion in 1 M HCl in the absence and presence of various additions of *R. chalepensis* L. oil using a gravimetric method. Various thermodynamic parameters for inhibitor adsorption on steel surface were estimated, discussed and the inhibition mechanism was suggested. It is expected to accumulate useful information on the adsorption and inhibition effect of *R. chalepensis* L. oil on steel in acid solution.

## 2. MATERIALS AND METHODS

### 2.1 Solution preparation

The solution 1M HCl was prepared by dilution of analytical grade 37% HCl with double distilled water. The solution tests are freshly prepared before each experiment by adding the oil directly to the corrosive solution. Experiments were carried out in triplicate to ensure the reproducibility.

### 2.2 Plant collection and essential oil extraction

*R. chalepensis* L. was were collected during April 2010 in Ain-defla, north Algeria at 280 m altitude. The aerial parts of the plant were air-dried in the laboratory at room temperature.

The essential oil used was obtained by steam distillation of the aerial part (stem and leaves) of *R. chalepensis* L. The oil obtained was a colourless liquid. Essential oil was stored in sealed vials protected from the light at 4 °C before analyses. The density of the oil obtained was 0.8492 g.cm<sup>-3</sup> and the relevant refractive index was 1.431. The oil sample was subsequently analyzed by GC and GC/MS.

#### 2.2.1 Gas chromatographic analysis

The analysis of the oil was carried out by HP5890 with FID, using a capillary column coated with 5% phenyl diméthyle polysiloxanne (25 m x 0.25 mm x film thickness 0.25 µm); column temperature, 40 to 240°C at 5°C/min. Injector temperature 220°C; detector temperature 250°C, volume injected was 0,1 µl of the oil dilute in 10% of hexane. Carrier gas was N<sub>2</sub> with 1 ml/min.

### 2.2.2 Gas Chromatography/Mass Spectroscopy

The oil was analyzed by GC/MS using a Perkin Elmer Clarus 500 equipped with a cross-linked 5% phenyl diméthyle polysiloxanne PE Elite capillary column (30m · 0.25 mm · film thickness 0.25 µm). Operating conditions: The carrier gas flow was 1 ml He/min. The injector and detector temperatures were 250°C and 280°C respectively. The column temperature was held at 60°C for 1 min, then raised from 60°C to 150°C at 15°C/min and from 150°C to 275°C at 5°C /min. The program was run in the split less mode with a mass range of 80–600 u, and the scan interval was 0.5 s. Detector voltage was set at 1.5 kV.

The identification of the components was performed on the basis of chromatographic retention indices and by comparison of the recorded spectra with computed data libraries [47].

### 2.3 Electrochemical tests

The electrochemical study was carried out using a EG&G potentiostat/galvanostat PAR 273A piloted by CorrIII software. This potentiostat was connected to a thermostated double-wall cell with three electrodes. A saturated calomel electrode (SCE) and platinum electrode were used as reference and auxiliary electrodes, respectively. The material used for constructing the working electrode was the same used for gravimetric measurements. The surface area exposed to the electrolyte is 0.64 cm<sup>2</sup>. Potentiodynamic polarization curves were plotted at a polarization scan rate of 1 mV/s. Before all experiments, the potential was stabilized at free potential during 30 min. The polarization curves are obtained from –800 to –200 mV at 298 K. The solution test is there after de-aerated by bubbling nitrogen. Gas bubbling is maintained prior and through the experiments.

The EIS measurements are carried out with a model 5210 analyzer controlled by Powersuite software. After the determination of the steady-state current at a corrosion potential, a sine wave potential, 10 mV peak to peak at frequencies between 100 and 10 mHz, was superimposed on the rest potential. Computer software automatically controlled the measurements performed at rest potentials after 30 min of exposure at 298 K. The impedance diagrams are given in the Nyquist representation. All experiments were repeated three times to monitor reproducibility.

### 2.4 Weight loss measurements

Metal plate of composition 0.13 % C, 0.32 % Si, 0.64 % Mn, 0.15 % Cu, 0.012 % S, 0.01 % P, 0.038 % Al, 0.081 % Cr, 0.011 % Mo, 0.083 % Ni, 0.01 % V, and Fe balance was cut into 2 × 1 × 0.02 cm<sup>3</sup> pieces for weight loss measurements. Prior to all measurements, the exposed area was mechanically abraded with 180, 320, 800, 1200 grades of emery papers.

The specimens are washed thoroughly with bidistilled water, degreased with ethanol and dried. Gravimetric measurements are carried out in a double walled glass cell equipped with a thermostated cooling condenser. The solution volume is 60 cm<sup>3</sup>. The immersion time for the weight loss is 6 h at 298 K.

### 3. RESULTS AND DISCUSSION

#### 3.1 Essential oil composition

The major components of *R chalepensis L.* oil are shown in Table 1. It was clear, that *R chalepensis L.* oil is constituted by five products as majority components.

**Table 1.** Major Chemical composition of *R. chalepensis L.* essential oil.

S/N°	Constituents	Tr (min)	% Compositions
1	(Z)-3-hexen-1-ol-acetate	6.76	0.3
2	p-Cymene	10.27	0.1
3	D-Limonene	10.38	0.1
4	2-Nonanone	11.97	1.1
5	Nonanal	12.29	1.0
6	1-Nonanol	13.96	0.6
7	2-Decanone	14.50	9.0
8	2-Undecanone	17.02	67.0
9	3-Undecanone	18.51	1.0
10	2-Dodecanone	19.17	4.0
11	2-Tridecanone	21.28	2.7
12	2-Phenyl-octanone	24.81	1.6
13	6-(3',5'-Benzodioxyl)-2-hexanone	27.55	6.3
14	8-(3',5'-Benzodioxyl)-2-octanone	31.04	0.5
Total		97	95.3

The main constituents were 2-Undecanone (67 %), 2-Decanone (9 %), 6-(3',5'-Benzodioxyl)-2-hexanone (6.3 %) and 2-Dodecanone (4 %).

#### 3.2 Effect of concentration

##### 3.2.1 Gravimetric measurements

The weight loss method is beneficial for monitoring inhibition efficiency due to its simple usage and reliability. The effect of *R. chalepensis L.* oil addition at different concentration on steel in acid medium (1M HCl) was studied by weight loss measurement at room temperature (298K) for 6 h immersion period.

The variation of the gravimetric parameters ( $W_{\text{corr}}$  and E %) of steel coupons in 1M HCl with and without the addition of various concentrations of the *R. chalepensis L.* oil is shown in Table 2. The value of the inhibition efficiency (E %) was determined using the equation (1).

$$E_G = \frac{W_{\text{corr}} - W'_{\text{corr}}}{W_{\text{corr}}} \times 100 \quad (1)$$

where  $W_{\text{corr}}$  and  $W'_{\text{corr}}$  are the corrosion rate in absence and presence of the inhibitor, respectively.

**Table 2.** Corrosion rate of steel in 1M HCl with and without *R. chalepensis L.* oil at various concentrations, and the corresponding inhibition efficiency

Inhibitor	Concentration (ml/L)	W (mg/cm <sup>2</sup> .h)	E (%)
Blank	0	0.21	/
<i>R. chalepensis L.</i> oil	0.5	0.1486	29
	1.5	0.1012	52
	2.5	0.05421	74

From the weight loss results, it's clear that the corrosion rate of steel in the blank is higher in comparison with the blank containing *R. chalepensis L.* The W decreased when the concentration of inhibitors. The addition of 0.5 ml. L<sup>-1</sup> *R. chalepensis L.* oil into the aggressive medium reduces this corrosion rate by 29 % and reaches 74 % at 2.5 ml. L<sup>-1</sup>. The inhibition efficiency of *R. chalepensis L.* oil increases as function of its concentration. This result suggests that an increase in oil concentration increases the number of inhibitor molecules adsorbed onto the steel surface and reduces the surface area that is available for the direct acid attack on the metal surface [20].

### 3.2.2 Polarization measurements

Potentiodynamic polarisation curves of steel in 1M HCl in the absence and presence of *R. chalepensis L.* oil at different concentrations at 298 K are presented in figure 2. The corrosion parameters including corrosion current densities ( $I_{corr}$ ), corrosion potential ( $E_{corr}$ ), cathodic Tafel slope ( $b_c$ ) and inhibition efficiency (E %) are listed in Table 3.

The inhibition efficiency is defined as follows:

$$E\% = \left(1 - \frac{I'_{corr}}{I_{corr}}\right) \times 100 \tag{2}$$

Where  $I_{corr}$  and  $I'_{corr}$  are current density in absence and presence of *R. chalepensis L.* oil respectively.

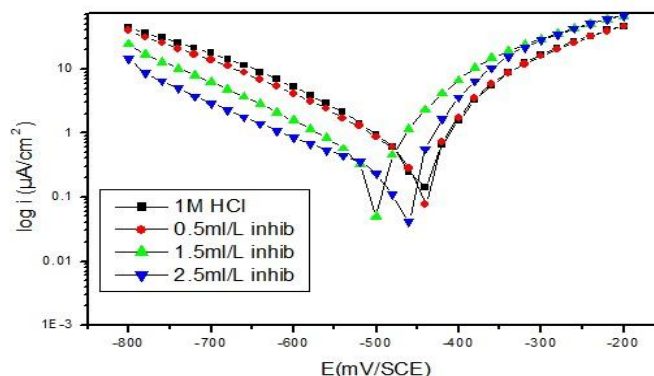


**Figure 1.** Potentiodynamic polarization curves of steel in 1M HCl in the presence of different concentrations of *R. chalepensis L.* oil.

**Table 3.** Electrochemical parameters of steel in 1M HCl solution without and with *R. chalepensis L.* oil at different concentrations.

Inhibitor	Concentration (ml/L)	$E_{corr}$ (mV)	$b_c$ (mV/dec)	$I_{corr}$ ( $\mu A/cm^2$ )	E%
Blank	0	-464	177	480	/
<i>R. chalepensis L.</i> oil	0.5	-467	180	374.4	22
	1.5	-534	167	254.4	47
	2.5	-439	175	139.2	71

As it can be noticed, both anodic and cathodic reactions of the steel corrosion electrodes were inhibited with the increase of oil concentration. This result suggests that the addition of *R. chalepensis L.* oil inhibitors reduced the anodic dissolution and also retarded the cathodic reaction by blocking the steel surface.

We also remark that the cathodic current-potential curves give rise to Tafel lines, which indicate that hydrogen evolution reaction is activation controlled. The cathodic Tafel slope values in the presence of *R. chalepensis L.* oil are different of that in its absence; we may deduce that this green inhibitor modifies the mechanism of the reduction process [48]

Additionally, From Table 3, it could be noted that E% increased with increasing inhibitor concentration, reaches 71 % at 2.5 ml/L. The results obtained from electrochemical are in good agreement with weight loss studies.

### 3.2.3 Electrochemical impedance spectroscopy measurements

The effect of inhibitor concentration on the impedance behavior of steel in 1 M HCl solution at 298K is presented in Figure 2. The curves show a similar type of Nyquist plots for steel in the presence of various concentrations of inhibitor.

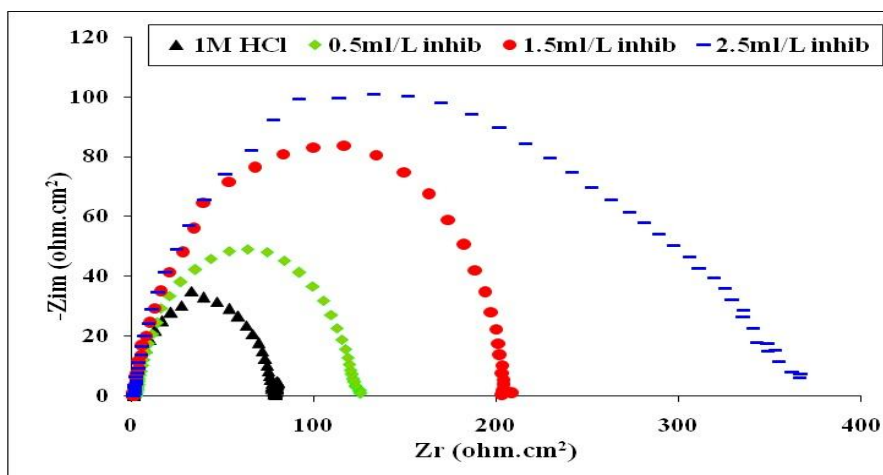


**Figure 2.** Nyquist plots of steel in 1 M HCl containing various concentrations of *R. chalepensis L.* oil at  $E_{corr}$  after 30 min of immersion.

The inhibition efficiency got from the charge transfer resistance is calculated by:

$$E_{R_t} \% = \frac{(R_t - R_t^0)}{R_t} \times 100 \quad (3)$$

Where  $R_t$  and  $R_t^0$  are the charge transfer resistances in inhibited and uninhibited solutions respectively.

The charge transfer resistance ( $R_t$ ) values are calculated from the difference in impedance at lower and higher frequencies, as suggested by Tsuru et al. [49]. The double layer capacitance ( $C_{dl}$ ) values were obtained at maximum frequency ( $f_{max}$ ), at which the imaginary component of the Nyquist plot is maximum and calculated using the following equation:

$$C_{dl} = \frac{1}{2\pi \cdot f_{max} \cdot R_t} \quad (4)$$

With  $C_{dl}$ : double layer capacitance ( $\mu\text{F}\cdot\text{cm}^{-2}$ );  $f_{max}$ : maximum frequency (Hz) and  $R_t$ : Charge transfer resistance ( $\Omega\cdot\text{cm}^2$ ).

The electrochemical impedance parameters derived from these investigations are mentioned in Table 4.

**Table 4.** Impedance parameters for corrosion of steel in 1 M HCl in the absence and presence of different concentrations of *R. chalepensis L.* at 298 K.

Inhibitor	Concentration (ml/L)	$R_t$ ( $\Omega\cdot\text{cm}^2$ )	$f_{max}$ (Hz)	$C_{dl}$ ( $\mu\text{F}/\text{cm}^2$ )	$E_{R_t}$ (%)
Blank	0	80.3	23.46	85	/
<i>R. chalepensis L.</i> oil	0.5	126.84	46.13	27	37
	1.5	204.52	77.23	10	62
	2.5	350.9	102.47	4	77

As it can be seen from Figure 2, impedance diagrams show a semi-circular appearance, indicating a charge transfer process mainly controls the corrosion of steel [50]. The existence of single semi-circle showed the single charge transfer process during dissolution which is unaffected by the presence of inhibitor molecules. Deviations from perfect circular shape are often referred to the frequency dispersion of interfacial impedance which arises due to surface roughness, impurities, dislocations, grain boundaries, adsorption of inhibitors, and formation of porous layers and in homogenates of the electrode surface [51-52].

From the impedance data, we notice an increase of the charge transfer resistance and decrease of the double layer capacitance with increasing inhibitor concentration. This phenomenon is generally related to the adsorption of organic molecules on the metal surface and then leads to a decrease in the local dielectric constant and/or an increase in the thickness of the electrical double layer indicate that *R. chalepensis L.* oil inhibits the corrosion rate of Steel by an adsorption mechanism [53]. The equivalent electrical circuit that may account for such behavior is represented in Figure 3

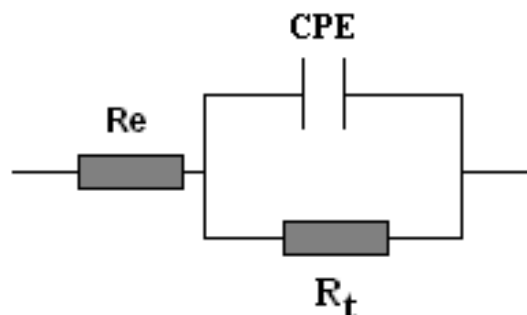


**Figure 3.** Equivalent circuit used to simulate the EIS diagram.

A comparison may be made between inhibition efficiency  $E$  (%) values obtained by different methods (weight loss, polarization curves and EIS methods). Figure 4 shows a histogram that compares the  $E$  (%) values obtained. One can see that whatever the method used, no significant changes are observed in  $E$  (%) values. We can then conclude that there is a good correlation with the three methods used in this investigation at all tested concentrations and that *R. chalepensis L.* oil is an efficient corrosion inhibitor.

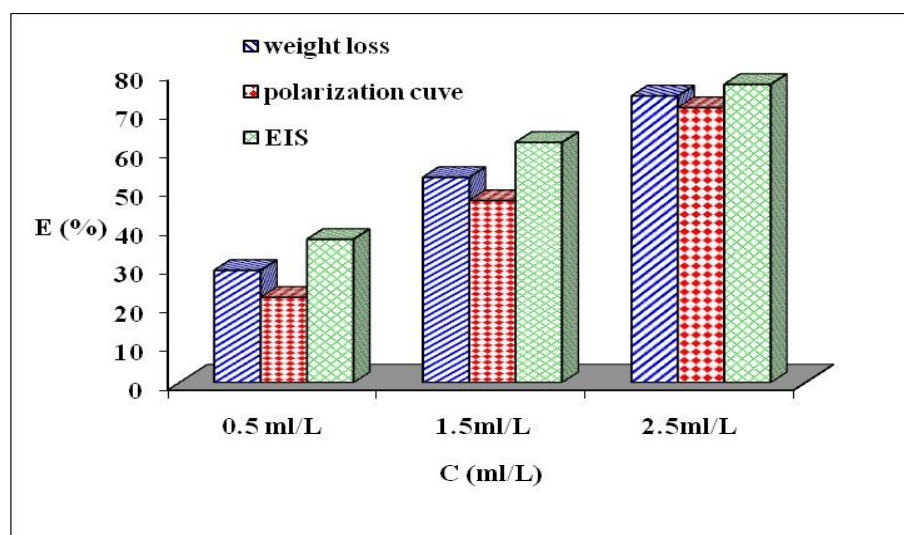


**Figure 4.** Comparison of inhibition efficiency ( $E$ %) values obtained by weight loss, polarization and EIS methods.

### 3.3 Effect of temperature

In order to study the effect of temperature on the inhibition efficiencies of *R. chalepensis L.* essential oil, weight loss measurements were carried out in the temperature range (308–338K) during 1 hour of immersion in absence and presence of inhibitor at optimum concentration. Table 5 shows the effect of temperature on the corrosion rate of steel in absence and presence of *R. chalepensis L.* oil at 2.5 ml/L.

**Table 5.** Effect of temperature on the steel corrosion in the presence and absence of 2.5 ml/L of *R. chalepensis L.* oil at 1 h

Temperature (K)	W(mg/cm <sup>2</sup> h)	W' (mg/cm <sup>2</sup> h)	E (%)
308	0.43	0.1204	73
318	1.49	0.4321	71
328	5.27	1.6337	69
338	13.62	3.6774	73

The results show that the inhibition efficiency (E %) is independent of temperature, showing that *R. chalepensis L.* oil is an efficient inhibitor in the range of temperature studied.

The activation parameters for the studied system ( $E_a$ ,  $\Delta H_a^*$  and  $\Delta S_a^*$ ) were estimated from the Arrhenius equation and transition state equation (Equation 5, 6) :

$$W = A \cdot \exp\left(-\frac{E_a}{R \cdot T}\right) \tag{5}$$

$$W = \frac{RT}{Nh} \exp\left(\frac{\Delta S_a^*}{R}\right) \exp\left(-\frac{\Delta H_a^*}{RT}\right) \tag{6}$$

where A is Arrhenius factor,  $E_a$  is the apparent activation corrosion energy, N is the Avogadro’s number, h is the Plank’s constant, and  $\Delta H_a^*$  and  $\Delta S_a^*$  are the enthalpy and the entropy changes of activation corrosion energies for the transition state complex. R is the perfect gas constant.

The apparent activation energy was determined from the slopes of Ln W vs 1000/T graph depicted in Figure 5

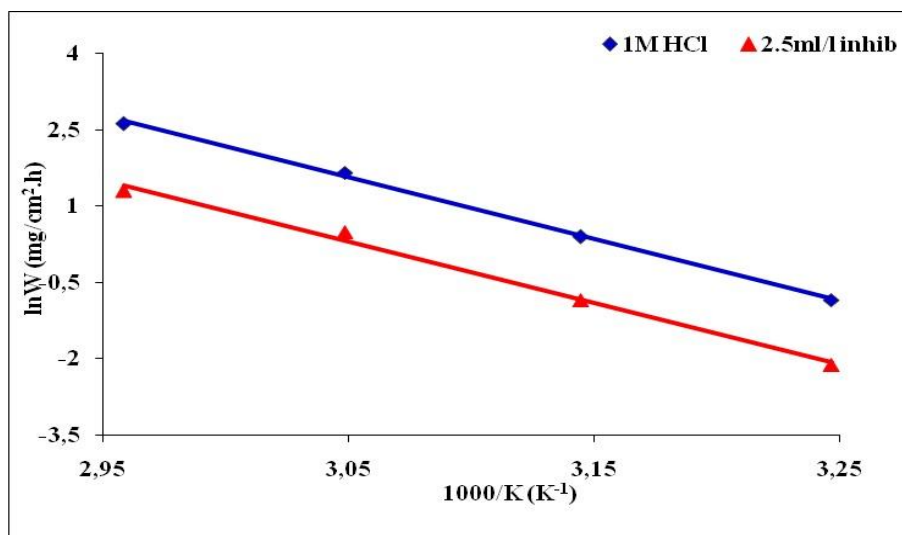


**Figure 5.** Arrhenius plots of steel in 1 M HCl with and without 2.5 ml/L *R. chalepensis L.* oil.

Figure 6 shows a plot of Ln (W/T) against 1/T of *R. chalepensis L.* oil. Straight lines are obtained with a slope of  $(-\Delta H_a^*/R)$  and an intercept of  $(\ln R/Nh + \Delta S_a^*/R)$  from which the values of  $\Delta H_a^*$  and  $\Delta S_a^*$  are calculated respectively (Table 6).

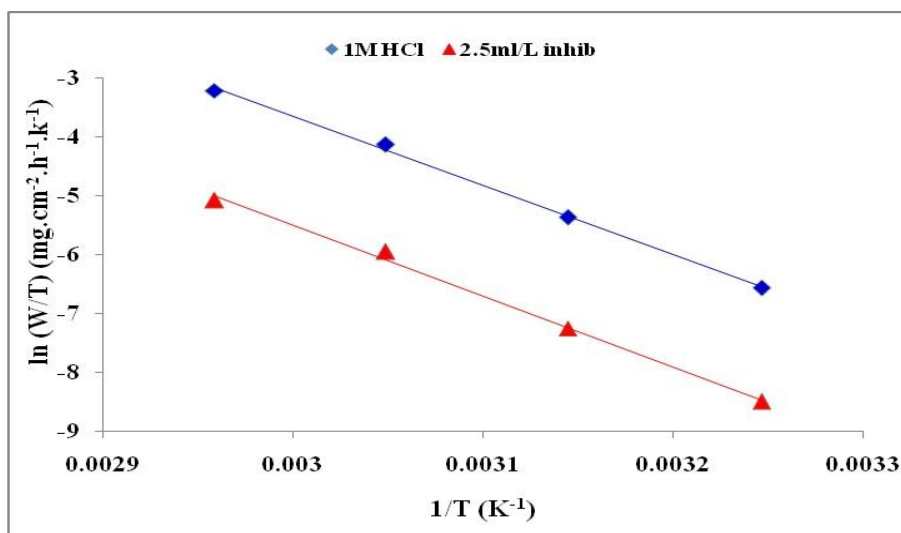


Figure 6. Relation between Ln (W/T) and 1/T at different temperatures.

Table 6. The values of activation parameters  $\Delta H_a^*$  and  $\Delta S_a^*$  for Steel in 1M HCl in the absence and the presence of 2.5 ml/L of *R. chalepensis L.* oil.

Inhibitor	$E_a$ (kJ/mol)	$\Delta H_a^*$ (kJ/mol)	$\Delta S_a^*$ (J/mol)	$E_a - \Delta H_a^*$ (KJ/mol)
Blank	100.83	98.35	407.53	2.48
<i>R. chalepensis L.</i> oil	103.55	101.06	396.29	2.49

From the following results, it can be concluded that:

- The increase in activation energy in presence of the inhibitor studied. This modification of value of  $E_a$  may be attributed to the change in the mechanism of the corrosion process in the presence of adsorbed inhibitor molecules [20]. The higher value of the activation energy of the process in an inhibitor’s presence when compared to that in its absence is attributed to its physisorption.

- The  $E_a$  and  $\Delta H_a^*$  values vary in the same way with the inhibitor concentration. This result permit to verify the known thermodynamic relation between  $E_a$  and  $\Delta H_a^*$  [54]:

$$E_a - \Delta H_a^* = RT \tag{7}$$

The calculated values are very close to RT which is equal 2.48 kJ mol<sup>-1</sup> at 305 K.

- The positive values of  $\Delta H_a^*$  show that the corrosion process is an endothermic phenomenon.

- The decrease of values of  $\Delta S_a^*$  show that the activated complex in the rate determining step represents an association rather than a dissociation step, meaning that a decrease in disordering takes place on going from reactants to the activated complex [55]

### 3.4 Adsorption considerations

Basic information on the interaction between the inhibitor and the mild steel can be provided by the adsorption isotherm. The adsorption of the inhibitors can be described by two main types of

interaction: physical adsorption and chemisorption's [56-58]. These are influenced by the chemical structure of the inhibitor, the type of the electrolyte and the charge and nature of the metal. Adsorption isotherms provide information about the interaction among adsorbed molecules themselves as well as their interactions with the metal surface. Surface coverage values were evaluated from the gravimetric measurements assuming a direct relationship between inhibition efficiency and surface coverage. The surface coverage values (defined as  $E/100$ ) were fitted to different adsorption isotherm models and the best results judged by the correlation coefficient ( $R^2$ ) were obtained with the Langmuir isotherm. According to this isotherm the surface coverage is related to concentration inhibitor  $C$  via:

$$\frac{C}{\theta} = \frac{1}{K_{ads}} + C \quad (8)$$

Where  $\theta$  is the surface coverage,  $C$  is the concentration,  $K_{ads}$  is the equilibrium constant of adsorption process. The plot of  $C/\theta$  against  $C$  is shown in Figure 7.

The plots of  $C/\theta$  versus  $C$  yielded straight lines for *R. chalpensis L.* oil with a very good correlation coefficient (0.979). This result indicates that the adsorption of compound under consideration on steel/acidic solution interface follows the Langmuir adsorption isotherm.

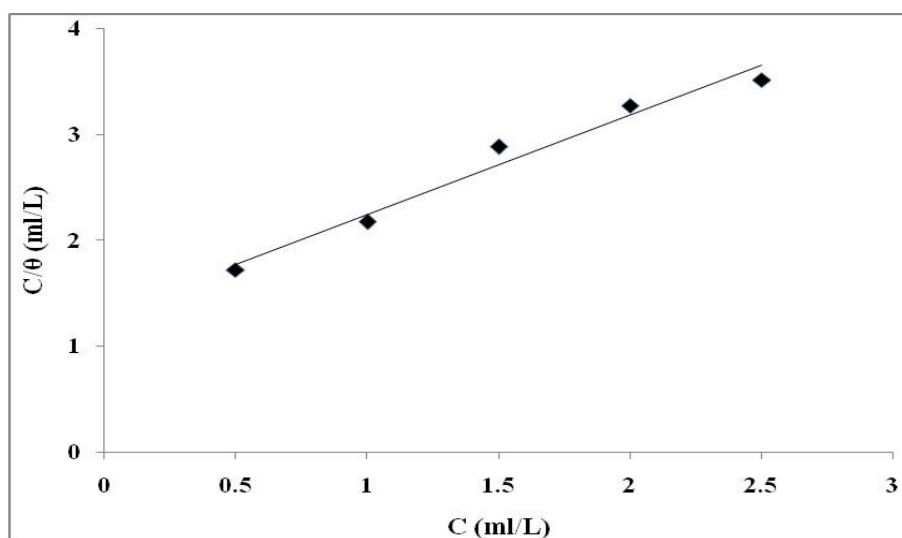


**Figure 7.** Langmuir adsorption isotherm model for *R. chalpensis L.* oil in 1M HCl

On the basis of characterization of *R. chalpensis L.* essential oil, we postulate that the major components act together by adsorption to ensure inhibition. Then, the inhibition is regarded as intermolecular synergistic effect of the various components of natural oil or essential oil. It is safely recommended to not determine  $\Delta G_{ads}$  values since the mechanism of adsorption remains unknown [59].

### 3.5 Suggested mechanism of corrosion inhibition

In hydrochloric acid medium, the metal surface is negatively charged due to the specifically adsorbed chloride ions on the metal surface.

In acidic solution, the oxygen atom of the major component (2-Undecanone) of the inhibitor can be protonated easily, due to high electron density on it, leading to positively charged inhibitor species. The adsorption can occur via electrostatic interaction between positively charged inhibitor molecules and negatively charged metal surface leading to physisorption of the inhibitor molecules. Further, co-ordinate bond may be formed between unshared e- pairs of unprotonated oxygen atom of the inhibitor and vacant d-orbitals of metal surface atoms [61].

#### 4. CONCLUSION

In this work, the inhibitive action of *R. chalepensis L.* oil, an inexpensive, eco-friendly, and naturally occurring substance, on the corrosion behavior of steel in 1 M HCl has been studied by using various methods. The results obtained are in good agreement and are given as follows.

- The major constituents of *R. chalepensis L.* oil were 2-Undecanone (67 %), 2-Decanone (9 %), 6 (3', 5'-Benzodioxyl)-2-hexanone (6.3 %) and 2-Dodecanone (4 %).
- The *R. chalepensis L.* oil provides a good inhibition of corrosion of steel in normal hydrochloric acid medium.
- The inhibition efficiency increases with increased *R. chalepensis L.* oil concentration to attain a maximum value of 77 % at 2.5 ml/L.
- The inhibition efficiency of *R. chalepensis L.* oil is independent of temperature.
- The values of apparent activation energy increases with the increase in the inhibitor concentration.
- Enthalpy of activation reflects the endothermic nature of steel dissolution process. Entropy of activation decreases with increasing inhibitor concentration; hence decrease in the disorder of the system.
- The adsorption of *R. chalepensis L.* oil on steel follows the Langmuir adsorption isotherm.
- The inhibitor can be adsorbed physically on the metal surface through oxygen atom of 2-Undecanone; the main constituent presents in *R. chalepensis L.* oil.
- The inhibition efficiencies of the *R. chalepensis L.* oil obtained from the polarization technique are in good agreement with the values obtained from the gravimetric measurements. This agreement among two independent techniques proves the validity of the results.

#### References

1. AH. Ostovari, SM. Peikari, SR. Shadizadeh, SJ. Hashemi, *Corros. Sci.* 51 (2009) 1935.
2. A. Hamdy, NS. El-Gendy, *Egypt. J. Petrol.* 22 (2013) 17.
3. A. Ousslim, A. Aouniti, K. Bekkouch, A. Elidrissi, B. Hammouti, *Surface Review and Letters.* 16 (2009) 787.
4. H. Zarrok, H. Oudda, A. Zarrouk, R. Salghi, B. Hammouti, M. Bouachrine, *Der Pharma Chemica.* 3 (2011) 576.
5. S. Kertit, B. Hammouti, *Appl. Surf. Sci.* 93 (1996) 59.

6. K. Tebbji, H. Oudda, B. Hammouti, M. Benkaddour, SS. Al-Deyab, A. Aouniti, *Res. Chem. Intermed.* 37 (2011) 985.
7. Z. Jiang, J. Wang, Q. Hu, S. Huang, *Corros. Sci.* 37 (1995) 1245.
8. F. Bentiss, M. Traisnel, L. Gengembre, M. Lagrenee, *Appl. Surf. Sci.* 52 (1999) 237.
9. SS. Abd El-Rehim, SAM. Refaey, F. Taha, MB. Saleh, RAJ. Ahmed RAJ, *Appl. Electrochem.* 37 (2001) 429.
10. A. Popova, E. Sokolova, S. Raicheva, M. Christov, *Corros. Sci.* 45 (2003) 33.
11. A. Popova, M. Christov, A. Vasilev, *Corros. Sci.* 49 (2007) 3290.
12. UJ. Ekpe, EE. Ebenso, UJ. Ibok, *J. W. Afr. Sci. Assoc.* 39 (1994) 13.
13. EE. Ebenso, UJ. Ibok, *Discov. Innov.* 10 (1998) 52.
14. S. Martinez, I. Stern, *J. Appl. Electrochem.* 31 (2001) 973.
15. A. Popova, M. Christov, S. Raicheva, E. Sokolova, *Corros. Sci.* 46 (2004) 1333.
16. KC. Emregul, M. Hayvali, *Mater. Chem. Phys.* 83 (2004) 209.
17. EE. Oguzie, EE. Ebenso, *Pigment Resin Technol.* 35, 30 (2006)
18. EE. Oguzie, *Corros. Sci.* 50 (2008) 2993.
19. EE. Ebenso, NO. Eddy, AO. Odiongenyi, *Portug. Electrochim. Acta.* 27 (2009) 13.
20. A. Khadraoui, A. Khelifa, H. Hamitouche, R. Mehdaoui, *Res. Chem. Intermed.* 40 (2014) 961.
21. A. Khadraoui, A. Khelifa, *Res. Chem. Intermed.* 39 (2013) 3937.
22. PC. Okafor, UJ. Ekpe, EE. Ebenso, EM. Umoren, KE. Leizou, *Bull. Electrochem.* 21 (2005) 347.
23. AY. El-Etre, M. Abdallah, ZE. El-Tantawy, *Corros. Sci.* 47 (2005) 385.
24. B. Hammouti, A. Melhaoui, S. Kertit, *Bull. Electrochem.* 13 (1997) 97.
25. EE. Oguzie, AI. Onuchukwu, PC. Okafor, EE. Ebenso, *Pigment. Resin. Tech.* 35 (2006) 63.
26. AM. Abdel-Gaber, BA. Abd-El-Nabey, IM. Sidahmed, AM. El-Zayady, M. Saadawy, *Corros. Sci.* 48 (2006) 2765.
27. SA. Umoren, IB. Obot, EE. Ebenso, PC. Okafor, O. Ogbobe, EE. Oguzi, *Anti-Corros. Mater. Meth.* 53 (2006) 277.
28. A. Chetouani, B. Hammouti, M. Benkaddour, *Resin & Pigment Technol.* 33 (2004) 26.
29. E. El Ouariachi, J. Paolini, M. Bouklah, A. Elidrissi, A. Bouyanzer, B. Hammouti, *Acta Metallurgica Sinica.* 23 (2010) 13.
30. M. Bendahou, M. benabdallah, B. Hammouti, *Pigm. Res. Techn.* 23 (2006) 95.
31. A. Bouyanzer, B. Hammouti, *Bull. Electrochem.* 20 (2004) 63.
32. L. Bammou, B. Chebli, R. Salghi, L. Bazzi, B. Hammouti, M. Mihit, *Green Chemistry Letters and Reviews.* 3 (2010) 173.
33. M. Benabdellah, B. Hammouti, M. Benkaddour, M. Bendahou, A. Aouniti, *Appl. Surf. Sci.* 252 (2006) 6212.
34. M. Bouklah, B. Hammouti, *Portug. Electrochim. Acta,* 24 (2006) 457.
35. O. Ouachikh, A. Bouyanzer, M. Bouklah, JM. Desjobert, J. Costa, B. Hammouti, *Surface Review and Letters.* 16 (2009) 49.
36. B. Zerga, M. Sfaira, Z. Rais, M. Ebn Touhami, M. Taleb, B. Hammouti, *Materiaux et Technique.* 97 (2009) 297.
37. A. Bouyanzer, B. Hammouti, *Pigm. Resin & Techn.* 33 (2004) 287.
38. A. Bouyanzer, B Hammouti, L Majidi, *Materials Letters.* 60 (2006) 2840.
39. L. Afia, R. Salghi, L. Bammou, Lh. Bazzi, B. Hammouti, L. Bazzi, *Acta Metallurg. Sinica,* 25 (2012) 10.
40. L. Afia, R. Salghi, E.H. Bazzi, A. Zarrouk, B. Hammouti, M. Bouri, H. Zarrouk, L. Bazzi, L. Bammou, *Research on Chemical Intermediates,* 38 (2012) 1707.
41. A. Belkassam, A. Zellagui, N. Gherraf, M. Lahouel, S. Rhouati, *Advances in Natural and Applied Sciences.* 5 (2011) 264.
42. N. Mohr, H. Budzikiewicz, BAH. El-Tawil, FKA. El-Beih, *Phytochemistry.* 21 (1982) 1838.
43. B. Juan, FR. Del Castillo, S. Migel. Angustifolin, *Phytochemistry.* 23 (1984) 2095.

44. SK. Raghav, B. Gupta, C. Agrawal, K. Goswami, HR. Das, *Journal of Ethnopharmacology*. 104 (2006) 234.
45. IN. Kuzovkina, Sz. Szarka, É. Héthelyi, E. Lemberkovics, É. Szöke, *Russian Journal of Plant Physiology*. 56 (2009) 846.
46. J. Mejrib, A. Manef, M. Mejria, *Industrial Crops and Products*. 32 (2010) 671.
47. RM. Adams, RA. Fleming, CC. Chang, BA. McCarl, C. Rosenzweig, *Climatic Change*. 30 (1995) 147.
48. S. Kertit, B. Hammouti, *Appl. Surf. Sci.* 93 (1996) 59.
49. T. Tsuru, S. Haruyama, B. Gijutsu, *J. Jpn. Soc. Corros. Eng.* 27 (1978) 573 .
50. H. H. Hassan, E. Abdelghani, M. A. Amin, *Electrochim. Acta*, 52 (2007) 6359.
51. O. Benalli, L. Larabi, M. Traisnel, L. Gengembra, Y. Harek, *Appl. Surf. Sci.* 253 (2007) 2130.
52. I. Epelboin, M. Keddam, H. Takenouti, *J. Appl. Electrochem.* 2 (1972) 71
53. E. McCafferty, N. Hackerman, *J. Electrochem. Soc.* 119 (1972) 146.
54. GK. Gomma, MH. Wahdan, *Mater. Chem. Phys.* 39 (1995) 209.
55. I. Langmuir, *J. Amer. Chem. Soc.* 39 (1917) 1848
56. L. Larabi, O. Benali, Y. Harek, *Port. Electrochim. Acta.* 24 (2006) 337.
57. L. Larabi, Y. Harek, M. Traisnel, A. Mansri, *J. Appl. Electrochem.* 34 (2004) 833.
58. O. Benali, M. Ouazene, *Arab. J. Chem.* 4, 443 (2011)
59. MA. Quraishi, R. Sardar, *J. Appl. Electrochem.* 33 (2003) 1163.

© 2014 The Authors. Published by ESG ([www.electrochemsci.org](http://www.electrochemsci.org)). This article is an open access article distributed under the terms and conditions of the Creative Commons Attribution license (<http://creativecommons.org/licenses/by/4.0/>).